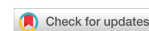


Research Article

Open Access



# High-gradient magnetic separation mechanism for separation of chalcopyrite from molybdenite

Pulin Dai<sup>1</sup>, Zixing Xue<sup>1</sup>, Xiaowei Li<sup>1</sup>, Yaxiong Jiang<sup>1</sup>, Nourhan Ahmed<sup>1,2</sup>, Jianwu Zeng<sup>1</sup>, Luzheng Chen<sup>1</sup>

<sup>1</sup>Faculty of Land Resource Engineering, Kunming University of Science and Technology, Kunming 650093, Yunnan, China.

<sup>2</sup>Faculty of Engineering, Assiut University, Assiut 71515, Egypt.

**Correspondence to:** Dr. Luzheng Chen, Faculty of Land Resource Engineering, Kunming University of Science and Technology, 253 Xuefu Road, Kunming 650093, Yunnan, China. E-mail: chluzheng@kust.edu.cn

**How to cite this article:** Dai P, Xue Z, Li X, Jiang Y, Ahmed N, Zeng J, Chen L. High-gradient magnetic separation mechanism for separation of chalcopyrite from molybdenite. *Miner Miner Mater* 2023;2:12. <https://dx.doi.org/10.20517/mmm.2023.12>

**Received:** 15 Jun 2023 **First Decision:** 28 Aug 2023 **Revised:** 14 Oct 2023 **Accepted:** 18 Oct 2023 **Published:** 23 Oct 2023

**Academic Editors:** Feifei Jia, Hyunjung Kim **Copy Editor:** Dong-Li Li **Production Editor:** Dong-Li Li

## Abstract

Removing molybdenite from chalcopyrite by flotation has long been a challenge due to their similar floatability as sulfide minerals. However, the difference in the magnetic susceptibility of the two minerals may be employed to address this challenge. Recently, pulsating high-gradient magnetic separation (PHGMS) has been reported effective as an environmentally friendly and economical strategy for separating chalcopyrite from molybdenite, but the mechanism of their magnetic difference is unclear. The current investigation employed crystal field theory and density functional theory calculations to theoretically elucidate the magnetic properties of these two minerals, and their difference was further demonstrated by experimental investigations. Under optimized conditions in a SLon-100 cyclic PHGMS separator, a chalcopyrite concentrate assaying 31.47% Cu and 0.44% Mo at 81.93% Cu and 5.56% Mo recoveries was produced from a pure chalcopyrite-molybdenite mixture that initially contained 26.29% Cu and 5.42% Mo. After the separation process, the Cu grade decreased to 15.06%, whereas the Mo grade increased to 16.22% in the nonmagnetic product. These findings have potential implications for the separation of chalcopyrite from molybdenite using PHGMS.

**Keywords:** Chalcopyrite, molybdenite, magnetic properties, crystal field theory, high gradient magnetic separation

## INTRODUCTION

Chalcopyrite ( $\text{CuFeS}_2$ ) and molybdenite ( $\text{MoS}_2$ ) are two common paragenetic sulfide minerals that are



© The Author(s) 2023. **Open Access** This article is licensed under a Creative Commons Attribution 4.0 International License (<https://creativecommons.org/licenses/by/4.0/>), which permits unrestricted use, sharing, adaptation, distribution and reproduction in any medium or format, for any purpose, even commercially, as long as you give appropriate credit to the original author(s) and the source, provide a link to the Creative Commons license, and indicate if changes were made.



typically found in porphyry copper deposits<sup>[1,2]</sup>, and they are difficult to separate by flotation due to their similar floatability. Therefore, large quantities of chemical reagents are usually required in the flotation process, which may bring cost problems and environmental issues<sup>[3]</sup>.

Pulsating high-gradient magnetic separation (PHGMS) is a physical separation method that employs the magnetic difference of minerals<sup>[4]</sup>, and it has been widely used in the field of mineral processing due to its high efficiency and environmental friendliness. Recently, some attempts of PHGMS was reported to separate chalcopyrite from sulfide minerals, such as arsenopyrite<sup>[5]</sup>, molybdenite<sup>[6]</sup>, and talc<sup>[7]</sup>. This approach is theoretically valid because the magnetic susceptibility of chalcopyrite is significantly higher than that of molybdenite. Therefore, they are separable through the PHGMS process, as present rather different magnetic properties. However, the mechanism responsible for the different magnetic properties of the minerals remains unknown due to the lack of suitable methods, and so far, no rational explanation has ever been reported.

To elucidate this mechanism, we proposed a model that explains the magnetic difference between chalcopyrite and molybdenite based on the splitting of d-orbitals in metal ions from the perspective of crystal field theory (CFT). Additionally, the electron spins were calculated using density functional theory (DFT). Finally, a PHGMS separator was used to perform the separation for a chalcopyrite-molybdenite mixture. The conclusions of this study have potential implications for separating chalcopyrite from molybdenite using PHGMS.

## METHODS AND SAMPLES

### DFT calculations for pure chalcopyrite and molybdenite

The DFT calculations were executed depending on the structures of chalcopyrite and molybdenite. This investigation utilized the first-principle DFT calculations of the CASTEP module to compute the crystal structures of chalcopyrite and molybdenite while presuming periodic boundary conditions, which belong to space groups  $I4\ 2d$  and  $P63/mmc$ . Then, the GGA function used in our calculations was approximated based on prior research, and the correlation energy obtained from the calculations was characterized using the gradient correction function called PW91<sup>[8]</sup>. To ensure convergence of the final energy, we set the truncation energy (energy cut-off) of the valence electron plane wave function to 400 eV. We selected the Fe  $3d^6\ 4s^2$ , S  $3s^2\ 3p^4$ , Cu  $3d^{10}\ 4s$ , and Mo  $4s^2\ 4p^6\ 4d^5\ 5s$  valence electrons to compute the pseudopotential of each atom. Notably, the Monkhorst-Park scheme was utilized to incorporate the Brillouin zone by conducting all calculations in reciprocal space. For the chalcopyrite and molybdenite slabs, k-points of  $2 \times 2 \times 2$  and  $5 \times 5 \times 1$  were respectively employed. During the calculations, a maximum force and stress of 0.1 eV/Å and 0.2 GPa, respectively, were permitted, and the convergence accuracy was set to  $1.0 \times 10^{-6}$  eV/atom. To increase the precision and dependability of the computations, it was necessary to consider the spin states of metal ions in both chalcopyrite and molybdenite. A diagram illustrating the geometrical supercell model is presented in [Figure 1](#).

### Overview of the chalcopyrite and molybdenite samples

This study employed highly purified chalcopyrite and molybdenite samples collected from Yunnan province, China. Both samples were ground and screened to a particle size of  $< 96\ \mu\text{m}$ . Chemical compositions and size distributions of both samples were displayed in [Tables 1](#) and [2](#), respectively.

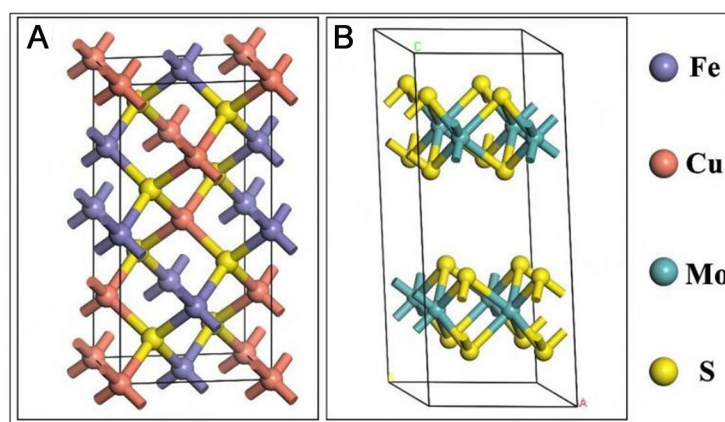
The particle size analysis results in [Table 2](#) indicate that both chalcopyrite and molybdenite are fine in size, with their mass weights smaller than 0.038 mm, exceeding 45%. Chalcopyrite and molybdenite particles

**Table 1. Chemical composition of the pure chalcopyrite and molybdenite**

Sample	Atomic concentration of elements (atomic, %)		
	Fe	Mo	Cu
Chalcopyrite	27.30	-	29.77
Molybdenite	-	54.13	-

**Table 2. Particle size analysis of pure chalcopyrite and molybdenite**

Particle size (mm)	Chalcopyrite weight (%)	Molybdenite weight (%)
+0.074	10.86	10.65
-0.074 + 0.045	33.87	28.58
-0.045 + 0.038	9.51	10.03
-0.038	45.76	50.74
Accumulation	100.00	100.00

**Figure 1.** Supercell model of (A) chalcopyrite and (B) molybdenite after geometry optimization.

with a size of +0.074 mm account for 10.86% and 10.65% of the respective samples. Additionally, particles with sizes between -0.074 and +0.038 mm represent 43.38% of chalcopyrite and 38.61% of molybdenite samples. According to the previous research results<sup>[5,6]</sup>, we selected particle sizes of -0.074 and +0.038 mm for the test of PHGMS.

### Description of PHGMS processes

A cyclic SLon-100 PHGMS separator was employed to carry out the separation test. As depicted in [Figure 2](#), The key components of the separator include a magnetic yoke, magnetic poles, excitation coils, and a pulsating mechanism<sup>[9]</sup>. To ensure the full immersion of the rod matrix, water was initially poured into the separation chamber, and then the pulsating mechanism was switched on to generate a pulsating flow. At the same time, a background magnetic induction was produced in the separation chamber by turning on the exciting current.

The mass weight, grade, and recovery of the magnetic product were used to evaluate the working performance<sup>[10]</sup>. The weights of the concentrate and tailings can be used to calculate the recovery in the capture test, as expressed in Eq. (1):

$$R = \frac{m_c}{m_T + m_c} \quad (1)$$

where  $R$  denotes the recovery (%),  $m_c$  denotes the mass of concentrates, and  $m_T$  denotes the mass of tailings. In addition, the recovery can be calculated using the weight and grade of the feed, concentrate, and tailings for each separation, as expressed in Eq. (2):

$$R = \frac{\beta(\alpha - \theta)}{\alpha(\beta - \theta)} \quad (2)$$

where  $R$  denotes the recovery (%),  $\alpha$ ,  $\beta$ , and  $\theta$  denote the grade of feed, concentrate, and tailings accordingly. To attain the results, each experiment was repeated three times, and the data was averaged out.

### Analysis of magnetic susceptibility by VSM for chalcopyrite and molybdenite

In this study, the magnetic properties of the two minerals were analyzed by using VSM (QUANTUM DESIGN PPMS-9) measurement techniques. The experiments were carried out under the conditions: 300 K (temperature), vibration frequency 40 Hz, vibration amplitude varying between 0.5 and 10 mm, sensitivity less than  $10^{-6}$  emu, magnetic induction intensity ranging from -2 to 2 T, and the maximum measured magnetic moment of 120 emu. These experimental conditions provide a deep understanding of the magnetic properties of the sample.

## RESULTS AND DISCUSSION

### Density of states analysis for metal ions in minerals

The density of states (DOS) was closely related to the atomic magnetic moment, which refers to the integral densities for both spin-up and spin-down states below the Fermi level of d-orbital in metal ions. This is expressed mathematically in Eq. (3)<sup>[5]</sup>:

$$m = \left[ \int_{E_0}^{E_F} DOS(\text{spin up}) dE - \int_{E_0}^{E_F} DOS(\text{spin down}) dE \right] \mu_B \quad (3)$$

where  $m$  represents the atomic magnetic moment, and  $E_F$ ,  $E_0$  represent the density of states at the Fermi energy level and the lower valence band, respectively. To elucidate the underlying reason for the magnetic susceptibility difference between chalcopyrite and molybdenite, an in-depth analysis of DOS curves for Fe in chalcopyrite and Mo in molybdenite was computed.

As illustrated in Figure 3, a noteworthy degree of asymmetry was observed in the DOS curve for Fe in chalcopyrite. In the range of -5 eV to Fermi level, a more negative magnetic moment was produced by Fe. While almost no magnetic moment was produced by Mo in molybdenite due to its highly symmetrical DOS curve. Consequently, chalcopyrite exhibited higher magnetic susceptibility than molybdenite due to their magnetic moment gap.

### Research of PHGMS experiments

#### *Independent capture analysis for chalcopyrite and molybdenite*

Capture analysis experiments were conducted using the following parameters: 50 g feed, 8.0-mm pulsating stroke, 3.0-cm/s feeding velocity, 2.0-mm-diameter matrix, 150, 200, and 250-rpm pulsating frequencies, and 0.8, 1.2, 1.4, and 1.6 T magnetic inductions.

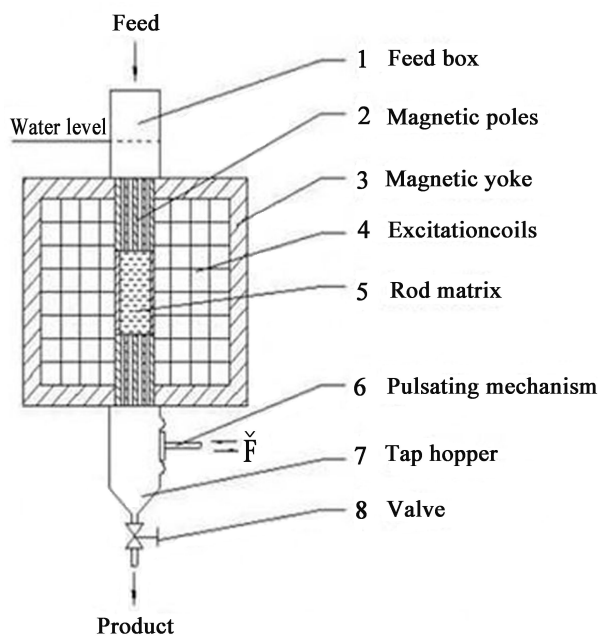


Figure 2. SLon-100 cyclic PHGMS separator. PHGMS: Pulsating high-gradient magnetic separation.

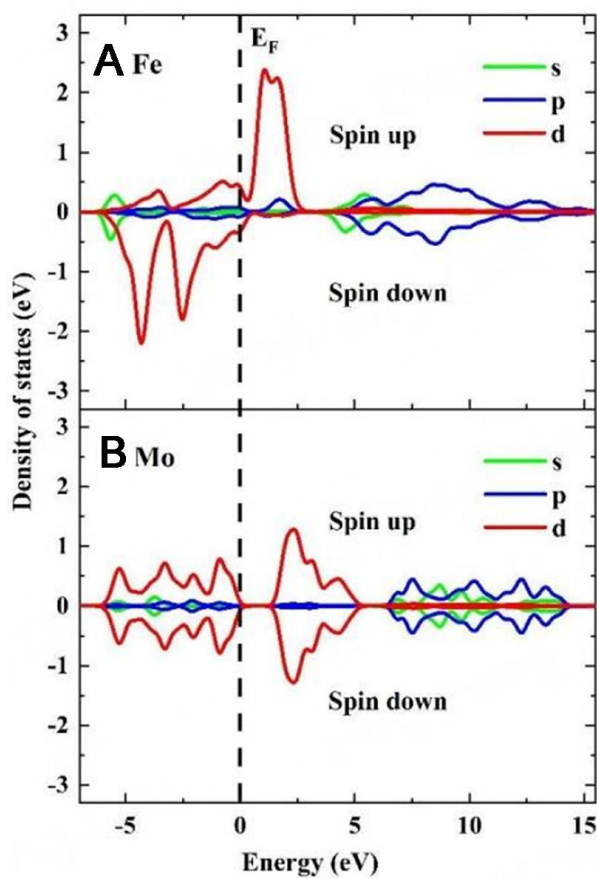


Figure 3. Density of states of Fe ions of (A) chalcopyrite and (B) molybdenite.

As depicted in [Figure 4](#), magnetic induction and pulsating frequency have significant impacts on the mass weight of the magnetic concentrate. However, the impact of the mineral type was even stronger. As illustrated in [Figure 4](#), a noticeably higher proportion of chalcopyrite was trapped onto the matrix as compared to molybdenite across all test conditions. This could be ascribed to the dissimilarities in their magnetic susceptibilities of the minerals, as the DFT calculations and CFT analysis indicated that the electrons of Fe ions have a higher spin state in chalcopyrite than the electrons of Mo ions in molybdenite.

According to [Figure 4](#), as the magnetic induction increased from 0.8 to 1.6 T, the mass weight of chalcopyrite increased, while that of molybdenite remained relatively stable. These results indicate that chalcopyrite has a stronger magnetic property than molybdenite as the magnetic induction increases at different pulsation frequencies.

### Separation test for chalcopyrite-molybdenite mixture

Based on the above capture analysis, it can be inferred that chalcopyrite and molybdenite can be effectively separated through the PHGMS process under appropriate test conditions. A separation test was performed using a mixture of pure chalcopyrite and molybdenite (mass ratio of 9:1) under optimized magnetic induction conditions (1.4 T).

The test results presented in [Table 3](#) demonstrate that chalcopyrite and molybdenite were able to be selectively separated by PHGMS. The chalcopyrite concentrate was produced by the magnetic separator assaying 31.47% Cu and 0.44% Mo at 81.93% Cu and 5.56% Mo recoveries, respectively. Furthermore, the Cu grade in the nonmagnetic product decreased to 15.06%, whereas the Mo grade increased to 16.22%.

To assess the performance of PHGMS for the separation of copper and molybdenum, we introduced two key parameters: the Mo reduction ratio in the copper concentrate product ( $R_{Mo}$ ) and the Separation Efficiency (SE)<sup>[6]</sup>. These parameters were calculated as follows:

$$R_{Mo} = \frac{\beta_{F,Mo} - \beta_{Cu,Mo}}{\beta_{F,Mo}} \quad (4)$$

$$SE = \frac{\beta_{Cu,Cu} \cdot (\beta_{F,Cu} - \beta_{Mo,Cu}) \cdot (\beta_{F,Mo} - \beta_{Cu,Mo})}{\beta_{F,Cu} \beta_{F,Mo} \cdot (\beta_{Cu,Cu} - \beta_{Mo,Cu})} \quad (5)$$

where  $\beta_{F,Cu}$ , and  $\beta_{F,Mo}$ ,  $\beta_{Cu,Cu}$  and  $\beta_{Cu,Mo}$ , are the Cu and Mo grades for copper-molybdenum concentrate and copper concentrate, respectively;  $\beta_{Mo,Cu}$  is the Cu grade of the nonmagnetic product. As calculated using Eqs. (4) and (5),  $R_{Mo}$  and SE are 91.88% and 76.61%, respectively. These results demonstrate the promising potential of using PHGMS as an eco-friendly and cost-effective method for chalcopyrite-molybdenite separation.

### VSM analysis for chalcopyrite and molybdenite

The magnetic properties of the two minerals were investigated through VSM analysis. [Figure 5](#) clearly shows the hysteresis loop, which describes how the magnetization of the mineral ( $M_s$ , emu/g) varies with the applied magnetic field ( $H$ , T). This hysteresis loop provides information about saturation magnetization intensity ( $M_s$ ), remanent magnetization ( $M_r$ ), and coercivity ( $H_c$ ).

As we know, the magnetic properties of minerals are determined by their crystal structure. It can be concluded from [Figure 5](#) that the magnetization value of chalcopyrite continues to increase when

**Table 3. PHGMS results of the separation test**

Products	Weight (%)	Grade (%)		Recovery (%)	
		Cu	Mo	Cu	Mo
Magnetic	68.44	31.47	0.44	81.93	5.56
Nonmagnetic	31.56	15.06	16.22	18.07	94.44
Feed	100.00	26.29	5.42	100.00	100.00

PHGMS: Pulsating high-gradient magnetic separation.

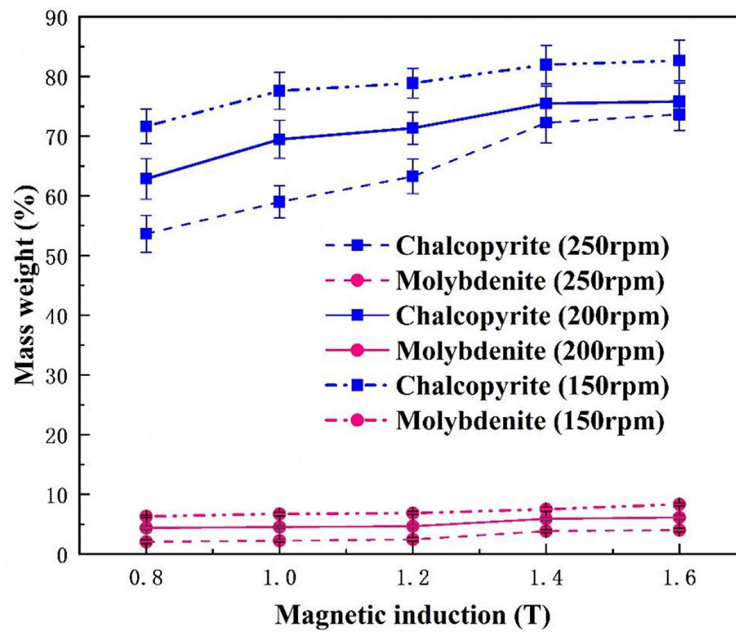


**Figure 4.** Effect of magnetic induction and pulsating frequency on the capture weight of pure chalcopyrite.

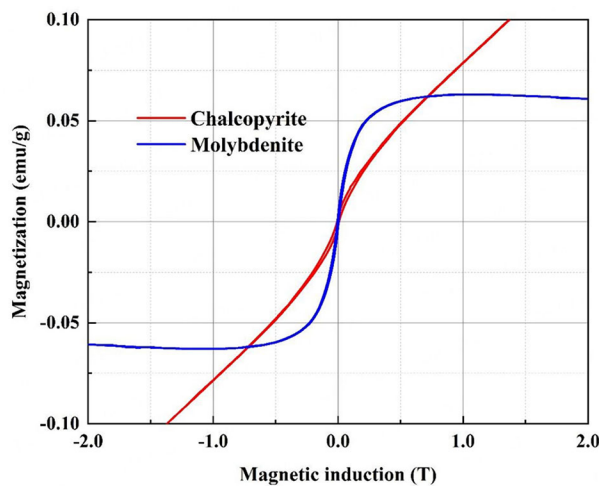


**Figure 5.** Magnetization intensity as a function of magnetic field for chalcopyrite and molybdenite.

molybdenite reaches saturation in magnetization ( $M_s$ ). The hysteresis loop of chalcopyrite forms an enclosed area with the coordinate axes. But molybdenite exhibits a narrow hysteresis loop that passes

through the zero point, indicating a linear relationship between its magnetization intensity and magnetic induction. Therefore, chalcopyrite exhibits higher remanent magnetization and coercivity compared to molybdenite.

### Electron configuration of d-orbital and magnetic moments of chalcopyrite and molybdenite

To further investigate the reasons for the difference in the magnetic susceptibility of chalcopyrite and molybdenite, CFT was employed to analyze the d-electron configuration of metal ions. Metal ions display diverse spin states in different crystal fields, which could significantly influence the properties of minerals<sup>[11]</sup>. In particular, chalcopyrite and molybdenite contain metal ions that possess diverse spin states that significantly influence their magnetic moments.

It is commonly known that the magnetic moment of matter stems from the spin and orbit of its electrons<sup>[12]</sup>. In particular, the magnetic moment for minerals is mainly determined by electron spin rather than electron orbit, which is greatly restricted by the ligand electric field.

Thereby, the magnetic moment of Fe in chalcopyrite and Mo in molybdenite was computed by Eq. (6), which only considered the electron spin effect.

$$\mu_s = \sqrt{n(n + 2)} \quad (6)$$

where  $\mu_s$  denotes the spin magnetic moment in Bohr magnetons (BM), and  $n$  denotes the number of single electrons.

In chalcopyrite, Fe<sup>3+</sup> ions are situated in a regular tetrahedral field, and its d-orbital electron configuration is d<sup>5</sup>, which results in a splitting energy ( $\Delta_o$ ) of its high energy level that is less than the electron pairing energy ( $P$ )<sup>[13]</sup>. Consequently, the electrons within the d-orbital of Fe<sup>3+</sup> tend to overcome  $\Delta_o$  and occupy the t<sub>2</sub>-orbital that has higher energy levels. This occurs after the orbital is occupied by two single electrons, as depicted in Figure 6.

Based on Eq. (6), it can be concluded that  $\mu_s$  is equal to 5.92 BM, indicating that electrons in the Fe ions in chalcopyrite exist in a high-spin state, which explains the source of magnetism for chalcopyrite.

In molybdenite, the d-orbital electron configuration of Mo is always d<sup>10</sup>. Therefore, regardless of whether the d-orbital splits, 10 electrons always occupy the five orbitals, as illustrated in Figure 7.

From Eq. (6), it is concluded that  $\mu_s = 0$  BM, indicating that electrons in the 3d-orbital of Mo<sup>4+</sup> in molybdenite exist in a low-spin state. Consequently, molybdenite possesses no magnetic moment and is difficult to capture effectively during HGMS, unlike chalcopyrite.

Fe ions in chalcopyrite occur within a regular tetrahedral field. As a result, electrons tend to surpass the energy splitting ( $\Delta t$ ), allowing the d<sup>5</sup> configuration to demonstrate a 5.92 BM magnetic moment and high-spin state following orbital splitting. In contrast, the electron configuration of Mo ions in molybdenite is d<sup>10</sup>. This implies that without the presence of a single unpaired electron in any orbit, the magnetic moment after d-orbital splitting is 0 BM. Consequently, chalcopyrite has a higher magnetic susceptibility than molybdenite.

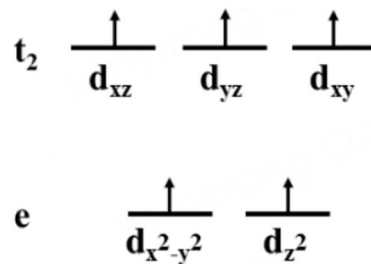


Figure 6. Spinning arrangement of  $\text{Fe}^{3+}$  in chalcopyrite.

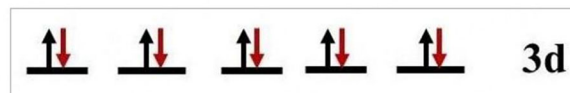


Figure 7. Spinning arrangement of  $\text{Mo}^{4+}$  in molybdenite.

## CONCLUSIONS

The higher magnetic susceptibility of chalcopyrite can be attributed to the high-spin state of electrons of Fe ions, which increases the magnetic moment. The Fe atoms in chalcopyrite are responsible for generating magnetic susceptibility in the mineral and contribute more negative magnetic moments that fall between the energy range of -5 eV and the Fermi level. In contrast, the Mo atoms in molybdenite exhibit high symmetry in this range, leading to the absence of magnetic susceptibility.

Strong evidence supporting the above explanation was provided by the successful selective separation of chalcopyrite from molybdenite under optimal PHGMS conditions. The chalcopyrite concentrate was generated by the cyclic PHGMS separator assaying 31.47% Cu and 0.44% Mo, at 81.93% Cu and 5.56% Mo recoveries, respectively, from a chalcopyrite-molybdenite mixture assaying 26.29% Cu and 5.42% Mo. Moreover, the Cu grade of the nonmagnetic molybdenite concentrate was reduced to 15.06%, with the Mo grade significantly increased to 16.22%. Meanwhile, Mo reduction ratio ( $R_{\text{Mo}}$ ) and separation efficiency (SE) were 91.88% and 76.61%, respectively.

## DECLARATIONS

### Authors' contributions

Data curation, formal analysis, investigation, methodology, software, visualization, writing - original draft, writing - review and editing: Dai P

Formal analysis, investigation, methodology, visualization, writing - review and editing: Xue Z

Conceptualization, funding acquisition: Jiang Y

Methodology, project administration: Li X

Resources, supervision, writing - review and editing: Ahmed N

Project administration: Zeng J

Conceptualization, investigation, methodology, resources, supervision, validation: Chen L

### Availability of data and materials

Not applicable.

### Financial support and sponsorship

This work was supported by the National Natural Foundations of China (52104255, 52264029), the High-Level Talent Recruitment Program of Yunnan Province (No. 140520210124), and the Basic Research

Program of Yunnan Province (202201AU070139).

### Conflicts of interest

All authors declared that there are no conflicts of interest.

### Ethical approval and consent to participate

Not applicable.

### Consent for publication

Not applicable.

### Copyright

© The Author(s) 2023.

## REFERENCES

1. Song S, Zhang X, Yang B, Lopez-mendoza A. Flotation of molybdenite fines as hydrophobic agglomerates. *Sep Purif Technol* 2012;98:451-5. [DOI](#)
2. Singer DA. Future copper resources. *Ore Geol Rev* 2017;86:271-9. [DOI](#)
3. Hirajima T, Mori M, Ichikawa O, et al. Selective flotation of chalcopyrite and molybdenite with plasma pre-treatment. *Miner Eng* 2014;66-8:102-11. [DOI](#)
4. Chen L, Ding L, Zhang H, Huang J. Slice matrix analysis for combinatorial optimization of rod matrix in PHGMS. *Miner Eng* 2014;58:104-7. [DOI](#)
5. Dai P, Yang J, Wei Z, Zeng J, Xue Z, Chen L. Magnetic properties of chalcopyrite and arsenopyrite for high-gradient magnetic separation with Crystal-Field Theory. *Miner Eng* 2022;189:107893. [DOI](#)
6. Chen L, Xiong T, Xiong D, et al. Pulsating HGMS for industrial separation of chalcopyrite from fine copper-molybdenun co-flotation concentrate. *Miners Eng* 2021;170:106967. [DOI](#)
7. Xian Y, Hong Y, Li Y, Li X, Zhang S, Chen L. Pulsating high-gradient magnetic separation of chalcopyrite and talc. *Miner Eng* 2022;178:107410. [DOI](#)
8. Perdew JP. Generalized gradient approximation for the fermion kinetic energy as a functional of the density. *Physics Letters A* 1992;165:79-82. [DOI](#)
9. Xiong D, Liu S, Chen J. New technology of pulsating high gradient magnetic separation. *Int J Miner Process* 1998;54:111-27. [DOI](#)
10. Zeng J, Tong X, Ren P, Chen L. Theoretical description on size matching for magnetic element to independent particle in high gradient magnetic separation. *Miner Eng* 2019;135:74-82. [DOI](#)
11. Chen J. The interaction of flotation reagents with metal ions in mineral surfaces: a perspective from coordination chemistry. *Miner Eng* 2021;171:107067. [DOI](#)
12. Buschow KHJ, de Boer FR. The magnetically ordered state. In: *Physics of magnetism and magnetic materials*. Boston: Springer US; 2003. p. 19-42. [DOI](#)
13. Chen J, Li Y. Orbital symmetry matching study on the interactions of flotation reagents with mineral surfaces. *Miner Eng* 2022;179:107469. [DOI](#)